Postsynthesis Vapor-Phase Functionalization of MCM-48 with Hexamethyldisilazane and 3-Aminopropyldimethylethoxylsilane for Bioseparation Applications

Antje Daehler,[†] Sasha Boskovic,[†,‡,§] Michelle L. Gee,[‡] Frances Separovic,[‡] Geoffrey W. Stevens,[†] and Andrea J. O'Connor*[,†]

Department of Chemical and Biomolecular Engineering and School of Chemistry, The University of Melbourne, Victoria 3010, Australia, and CSIRO Manufacturing and Infrastructure Technology, Private Bag 33, Clayton South MDC, Victoria 3169, Australia

Received: March 7, 2005; In Final Form: May 31, 2005

MCM-48 was surface modified via vapor-phase reactions with hexamethyldisilazane (CH_3-MCM-48) and 3-aminopropyldimethylethoxysilane (NH_2-MCM-48). ^{29}Si NMR confirmed that the resulting materials contained covalently attached trimethylsilane and 3-aminopropyldimethylsilane moieties, both important functionalities for bioseparation applications. The surface coverage was ∼1.8 and 0.9 groups per nm^2, respectively. The X-ray diffraction patterns and the narrow pore size distributions obtained from the gas sorption isotherms showed that the modified materials retained the characteristic pore structure of the underlying MCM-48 material. CH_3-MCM-48 exhibited significantly improved hydrolytic stability over the unmodified MCM-48 under the aqueous conditions tested, whereas NH_2-MCM-48 appeared to be less stable than the unmodified MCM-48. The decrease in stability is most likely due to the nature of the attachment of the 3-aminopropyldimethylsilane moiety, where the conversion of surface silanol groups is limited by H bonding with the amino end, leading to a 50% lower surface concentration and resulting in an increased likelihood of nucleophilic attack on the silica surface, enhancing the rate of hydrolysis. Hexamethyldisilazane thus appears to be a superior functional group for modifying the MCM-48 surface.

1. Introduction

Porous solids such as microporous zeolites are used as adsorbents, catalysts, and catalyst supports, owing to their high surface areas and significant pore volumes. However, their applications are limited by their small pore openings.[1] In 1992, researchers at Mobil reported the synthesis and properties of the M41S mesoporous silicates, a new class of synthetic materials, which extended the pore sizes into the mesoporous range.[2,3] These materials are remarkable in that they can be synthesized with narrow adjustable pore size distributions in the range of 1.5−10 nm, and they are rigid structures with high specific pore volumes and large specific surface areas, in excess of 700 m^2/g.[2,3] Their pores can be ordered in different regular arrays, hexagonal (MCM-41), lamellar (MCM-50), or cubic (MCM-48). MCM-41 consists of a uniform hexagonal array of linear pores, arranged in a honeycomblike structure.[4] MCM-48 is a 3D,[5,6] highly interwoven and branched array.[7,8] Most interest has focused on the hexagonal MCM-41 with its unconnected, unidimensional pores, attributes desirable in some applications such as a model mesoporous adsorbent to test gas adsorption theories. However, for the applications of catalysis and separation, the MCM-48 pore system is generally regarded as more advantageous. MCM-48 is expected to provide better access to the pores, more favorable mass transfer kinetics, and pore blockages are less likely.[6,8,9]

One pitfall in the application of mesoporous molecular sieves is structural damage that is sustained when in contact with moist air or water vapor[1,10−12] and upon storage at ambient conditions.[13] This susceptibility to moisture and the resulting structural collapse has been reported to be greater for MCM-48 than for MCM-41.[11] This structural degradation is a serious problem in the application of mesoporous molecular sieves as adsorbents for bioseparations because the medium for such separations is aqueous and it is important that structural integrity is retained throughout repeated adsorption and regeneration cycles, generally performed around room temperature. Recent work has shown that the M41S materials are modified by prolonged exposure to water and water vapor, showing decreased structural regularity and a loss of uniformity in pore shape, size and volume.[10,14−19] The hydrolysis of siloxane bridges (Si−O−Si bonds) has been identified as the main cause of this structural damage. This mechanism has been confirmed by the increase of the Q^3 (silanol group) signal by ^{29}Si NMR following contact with water vapor overnight.[19] It is believed that the hydrolysis takes place at siloxane bridges on the surface that have energetically strained bond angles. These siloxane groups are formed from the condensation of neighboring silanol groups upon calcination.[13,16,20−22] The formation of strained siloxane bridges is influenced by the synthesis conditions (e.g., silica precursor, pH) and treatment of the materials. Efforts to increase the hydrothermal stability of these materials often involve strategies that facilitate a relaxation of the framework structure,[13] postsynthesis restructuring,[23] the use of salt solutions during synthesis,[24,25] or the use of nonionic surfactant templates.[21]

Another approach to the optimization of mesoporous molecular sieves for separations is their surface functionalization. Functionalization by either co-condensation of organic species during synthesis or subsequent surface modification permits the tuning of surface properties and could thus provide higher

* Corresponding author: Tel: +61 3 8344 8962. Fax: 61 3 8344 4153. E-mail: andreajo@unimelb.edu.au.
† Department of Chemical and Biomolecular Engineering.
‡ School of Chemistry.
§ CSIRO Manufacturing and Infrastructure Technology.

10.1021/jp0511799 CCC: $30.25
Published on Web 08/06/2005

selectivity for specific separation processes,[26] while also potentially increasing stability to hydrolysis.[27] Although it is often easier to ensure uniform surface coverage with co-condensation, the products obtained by postsynthesis grafting are often structurally better defined and hydrolytically more stable. Control of the pore sizes is also achieved more easily using chemical grafting.[26,28]

Two potentially important functional groups for bioseparations are hydrophobic and amino groups. Hydrophobic surface modifiers are of interest because they increase the selectivity of the adsorbents for molecules with hydrophobic regions, which include many biological molecules, and have also been shown to increase the stability of mesoporous silica materials in aqueous solutions.[11,18,19,26,27,29,30] Amino functionalization is of interest because the charge on these surface groups is pH-dependent, so there is the potential to tune them to selectively target oppositely charged species. More importantly, the highly reactive amino group can be utilized as, essentially, a chemical anchor to which other species can be chemically attached.[31]

One method for hydrophobing the surface of mesoporous molecular sieves is by the chemical grafting of alkyltrichlorosilanes to the suface hydroxyl groups. Most commonly, this reaction is performed in solution using nonpolar solvents. However, studies performed on flat silica surfaces have shown that, for many alkyltrichlorosilanes, the quality of surface modification using this method is critically dependent on the level of surface water on the silica, a factor that is difficult to control.[32−34] An alternative to the more commonly used silanes are disilazanes that react with the surface hydroxy groups of silica upon condensation of the disilazane on the silica surface from the vapor phase. The successful chemical attachment of hexamethyldisilazane (HMDS) to surface hydroxyl groups of flat silica surfaces via this procedure has been demonstrated using infrared spectroscopy.[35] Several different disilazanes have been investigated for reaction with MCM-41, resulting in a surface coverage of 0.74−1.85 silyl groups per nm^2.[36] These silylating agents were found to be very effective for the modification of mesoporous materials because of their relatively slow monofunctional surface reaction and ease of desorption of the ammonia byproduct.

For amino functionalization of silica, aminopropylsilanes have been popular silanating agents although, as for the alkyltrichlorosilanes, the removal of trace quantities of water is crucial for the prevention of polymerization on the surface.[31] MCM-48 has been functionalized with 3-aminopropyltriethoxysilane, 3-aminopropyltrimethoxysilane, and [3-(2-aminoethylamino)propyl] trimethoxysilane in solution reactions from nonpolar solvents.[37−39] However, examination of the X-ray diffraction patterns reveals that, as a result of this surface reaction, the characteristic cubic peaks associated with MCM-48 have broadened and the intensities of higher angle peaks have decreased significantly, indicating loss of long-range order of the material. The monoalkoxysilane, 3-aminopropyldimethylethoxysilane, has a greater vapor pressure than the more commonly used trialkoxysilane, 3-aminopropyltriethoxysilane, and has been shown to covalently attach to the surface of silica in a vapor-phase reaction.[31]

In this study, we examine the postsynthesis vapor-phase functionalization of MCM-48 with hexamethyldisilazane (HMDS), performed to provide hydrophobic functionality to the surface of the material for the prevention of hydrolysis. We also examine postsynthesis vapor functionalization with 3-aminopropyldimethylethoxysilane (APDMES) for adding amino surface functionality. The materials were characterized via gas sorption analysis and X-ray diffraction to determine the impact of the surface modification on the structure of the MCM-48 material. The nature of the chemical attachment was determined via ^{29}Si and ^{13}C NMR. After functionalization, the stability of the materials was determined by immersion in aqueous buffer for up to 40 days to simulate the conditions to which these materials would be subjected in bioseparation applications such as peptide purification.

2. Materials and Methods

2.1. MCM-48 Synthesis. A method described by Schmidt et al.[40] was used for the synthesis of MCM-48. Sodium hydroxide (13.4 g, NaOH, AnalR, 99%) was dissolved in distilled water (340 g). Tetraethyl-ortho-silicate (144.4 g, TEOS, Fluka, ≥99%) was added to the solution while stirring. After five minutes, 556 g of aqueous cethyltrimethylammonium chloride solution (CTAC, 25 wt %, Aldrich) was added and the resulting gel was stirred for another 15 min. The gel was then loaded into a polypropylene bottle, which in turn was contained in a stainless steel autoclave, and heated in an oven for 72 h at 100 °C without stirring. After cooling to room temperature, the precipitate was collected, washed extensively with distilled water and then dried in air at ambient temperature. The dried material was placed in a muffle furnace under flowing nitrogen for calcination. The furnace was heated at a rate of 2 °C per minute to 540 °C. The calcination of the material was continued at 540 °C for 1 h in a stream of flowing nitrogen followed by 6 h in air. After calcination, the samples were separated into particle size fractions by sieving and the fractions between 106 and 600 μm were stored in a desiccator until further use.

2.2. Characterization. Nitrogen adsorption and desorption isotherms were measured at 77 K, using a Micromeritics (Norcross, USA) ASAP 2000. Prior to analysis, the samples were outgassed overnight at 150 °C under vacuum for the surface modified samples and at 250 °C for the unmodified samples. BET surface areas[41] were calculated using adsorption data recorded at relative pressures $p/p_0 = 0.05-0.2$, based on the measured weight of the material. The single point total pore volume was derived from the amount of gas adsorbed at a relative pressure of $p/p_0 \approx 0.99$.[42] BJH pore size distributions[43] were obtained from the adsorption branch of the isotherm using Halsey's thickness equation.[44]

Powder X-ray diffraction (XRD) of the material was performed using a Philips (Eidenhoven, The Netherlands) PW 1800 X-ray diffractometer (40 kV, 30 mA, step size 0.02°, count time 5 s, Cu Kα radiation). The XRD patterns were normalized to show the same intensity for the main peak for ease of comparison.

Nuclear magnetic resonance (NMR) analysis was performed on Varian (Palo Alto, USA) 300 NMR spectrometers operating at 75.45 MHz for ^{13}C and 59.60 MHz for ^{29}Si. Acquisition and processing of data were performed using Varian software. The ^{13}C and ^{29}Si NMR of liquids were recorded as static spectra (without spinning). The ^{13}C and ^{29}Si solid-state spectra were recorded by magic angle spinning (MAS) at ∼6 kHz to enhance resolution.[45] The ^{29}Si solid-state spectra were acquired using a MAS probe with a silicon-free stator; all other spectra were collected using an aluminum-free stator. A proton decoupling power of ∼70 kHz and a sweep width of 40 kHz for ^{29}Si and 50 kHz for ^{13}C were used. A line broadening of 60 Hz for ^{29}Si and 75 Hz for ^{13}C was applied. Solid samples were analyzed in a 5-mm zirconia rotor and liquid samples in a 5-mm glass tube. ^{13}C spectra were obtained using both single pulse (SP) and cross

polarization (CP) techniques. It is necessary to ensure that all silica species are equally excited by the radio frequency pulse in order to obtain quantitative information from the ^{29}Si MAS NMR spectra. Therefore, the spectra were collected in single pulse mode only, without cross polarization because the CP mode discriminates against silica nuclei isolated from protons.[46] Furthermore, the Q^4 atoms relax more slowly than the Q^3 silicon nuclei, and a suitably long recycle time between pulses needs to be chosen to allow complete relaxation.[47] In this work, this was achieved by using a $\pi/4$ pulse of 2 μs to reduce delays and a 60-s recycle time. Typically, ~900 scans were collected for the ^{29}Si solid-state MAS NMR spectra. ^{13}C SP and CP experiments were performed using a $\pi/2$ pulse width of 4.7 μs with a recycle time of 5 s (SP) or 3 s (CP) and a 3-ms contact time. Depending on the intensity of the signal, 4000−27 000 scans were collected.

2.3. Surface Modification. The surface modification reactions were performed in a purpose-built vapor-phase-reaction apparatus.[27]

Modification with HMDS: MCM-48 was surface modified by vapor-phase reaction with hexamethyldisilazane (HMDS, Merck, 98%). Note that the resulting modified material is referred to as CH_3-MCM-48, for convenience. The HMDS was treated by a freeze−thaw method prior to the reaction to remove any dissolved gases. To remove any adsorbed water, we heated the MCM-48 slowly under vacuum (<0.02 atm) to 350 °C and held at this temperature for a minimum of 8 h. The system was then isolated from the vacuum pump and the valve separating the vessel containing the HMDS from the rest of the system was opened, so that HMDS vapor could enter the reaction chamber. Condensation of HMDS onto the surface and in the pores of MCM-48 was allowed to take place while the reaction chamber cooled to room temperature. It is this condensation that results in surface silylation,[35] as described above. After at least 16-h contact between the MCM-48 and the condensed HMDS, the chamber was evacuated to remove the NH_3 byproduct and any unreacted HMDS and the resulting CH_3-MCM-48 was recovered and stored in a desiccator.

Modification with APDMES. The procedure used for surface amino-functionalization of MCM-48 has been described previously by White et al.[31] Note that the resulting modified material is referred to as NH_2-MCM-48, for convenience. Briefly, the MCM-48 was held under vacuum (<0.02 atm) at ~350 °C for a minimum of 8 h. The sample was then allowed to cool to room temperature while the vacuum was maintained. After cooling, the MCM-48 was isolated from the vacuum system and the APDMES vapor was introduced. The subsequent condensation of APDMES onto the surface and in the pores of MCM-48 facilitates the surface silylation reaction, as for the reaction with HMDS. A period of 2 days in contact with the condensate was allowed. At the end of this reaction period, the reactor was evacuated to remove the reaction byproduct (ethanol) and any unreacted APDMES, and then the NH_2-MCM-48 was recovered and stored in a desiccator.

For CH_3-MCM-48 and NH_2-MCM-48, several batches were prepared (ranging in size from 1 to 2 g), which showed very similar nitrogen sorption isotherms. Hence, the individual batches of each material were combined for further characterization and stability testing.

2.4. Stability Testing. The stability of MCM-48, CH_3-MCM-48, and NH_2-MCM-48 on exposure to aqueous solution was tested by immersing ~160 mg of each material in 10 mL of 0.05 M 2-(N-morpholino)-ethane-sulfonic acid (MES) buffer at pH 6. The MES buffer solution was prepared using MES hydrate (99.5%; Sigma, St Louis, MO) and MES sodium salt (Sigma, 99%). It was necessary to pre-wet the hydrophobically modified MCM-48 (CH_3-MCM-48) with 0.5 mL of AR grade ethanol to exclude air from the pores, before introducing the material to the aqueous buffer solution. The materials in buffer were shaken manually to ensure initial mixing but not further agitated during the contact period. Different samples of each material were immersed in buffer solution for periods of 1, 7, 14, and 40 days, respectively. The samples were then recovered by filtration and left to dry overnight at ambient conditions then transferred into a desiccator and left to dry further for a week.

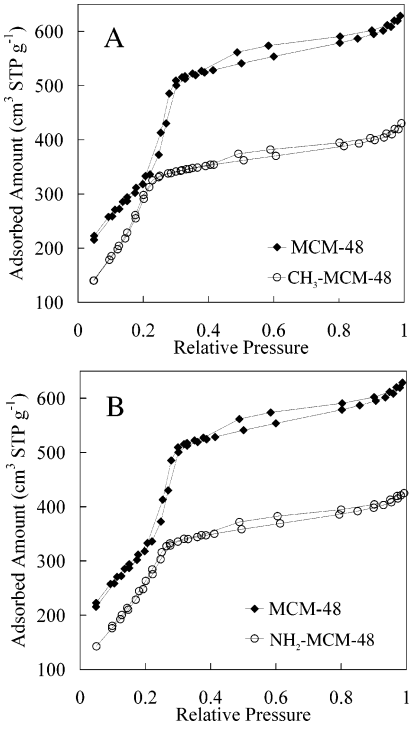

Figure 1. Nitrogen sorption isotherms for (A) CH_3-MCM-48 and (B) NH_2-MCM-48.

TABLE 1: Gas Sorption Parameters Determined for Unmodified and Functionalized MCM-48

sample	single point pore volume (cm^3/g)	peak position in BJH pore size distribution (nm)	BET surface area (m^2/g)
MCM-48	0.973	2.18	1181
CH_3-MCM-48	0.666	1.72	1225
NH_2-MCM-48	0.657	1.99	1000

3. Results and Discussion

The sorption isotherms for CH_3-MCM-48 and NH_2-MCM-48 are presented in Figure 1a and b, respectively. The sorption isotherm for unmodified MCM-48 is also shown in these figures for comparison. Note that the form of the sorption isotherms is not affected by surface functionalization. Another observation from this data is that surface functionalization leads to a significant decrease in the amount of nitrogen adsorbed, implying a decrease in pore volume. Both these results imply that surface functionalization had indeed occurred inside the MCM-48 pores, so reducing pore volume, and the functionalization was uniform such that the pore structure remained in tact. After functionalization, the isotherms retained the characteristic step between relative pressures of 0.2 to 0.3, although it was somewhat less pronounced than that for unmodified MCM-48. The step, characteristic of a narrow pore size

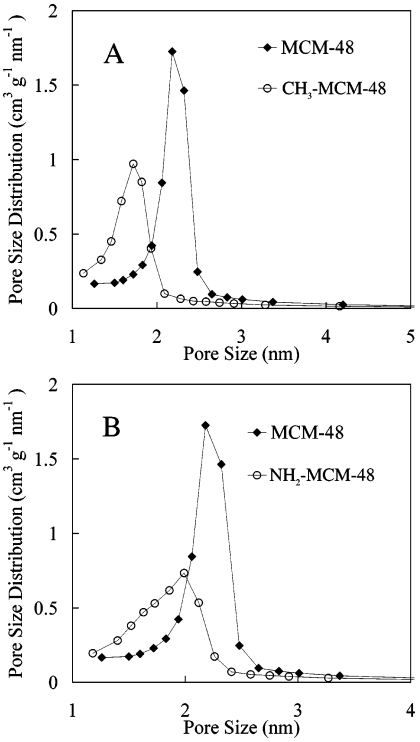

Figure 2. BJH pore size distributions for (A) CH_3-MCM-48 and (B) NH_2-MCM-48.

distribution, was shifted to slightly lower relative pressures, also indicative of a smaller average pore diameter.

As stated above, the volumes of nitrogen adsorbed per gram of material decreased significantly after surface modification of MCM-48 (see Table 1). Functionalization with HMDS resulted in a 31% drop in the single point pore volume. For a given amount of material, surface modification results in an increase in the material's weight, which will therefore reduce the specific material properties, including the single point pore volume and the nitrogen sorption isotherm itself. Analysis of ^{29}Si MAS NMR data (discussed later) attested to an increase in weight of about 26% because of the attachment of trimethylsilane groups. Thus, the observed change in the pore volume can be attributed to both the reduction in the pore diameter and the increase in sample weight. Similarly, for NH_2-MCM-48 a 32% reduction in the single point total pore volume was noted upon surface modification, with quantitative analysis of ^{29}Si MAS NMR data indicating an increase in weight of 23% due to the 3-aminopropyldimethylsilane groups. Interestingly, the BET surface area of CH_3-MCM-48 was higher than that of MCM-48, possibly because of an increase in surface roughness after surface modification.[48]

Figure 2 shows the BJH pore size distributions for modified and unmodified MCM-48. Although the BJH method is known to underestimate the pore size of M41S materials[49] and a statistical thickness equation specific to the surface nature of each differently functionalized material should strictly be used in calculations, this simple model is useful for comparison purposes. Note that the form of this distribution also did not change after surface modification with HMDS. This confirms that CH_3-MCM-48 is structurally similar to MCM-48. There was, however, a translation of the BJH distribution after surface modification indicative of a reduction in pore size. The peak in the distribution was shifted by ~0.5 nm. Zhao et al. observed that for MCM-41, the pore size decreased by 0.65 nm after attachment of trimethylsilane moieties to the surface.[50] One would expect the reduction in pore size to be twice the fully

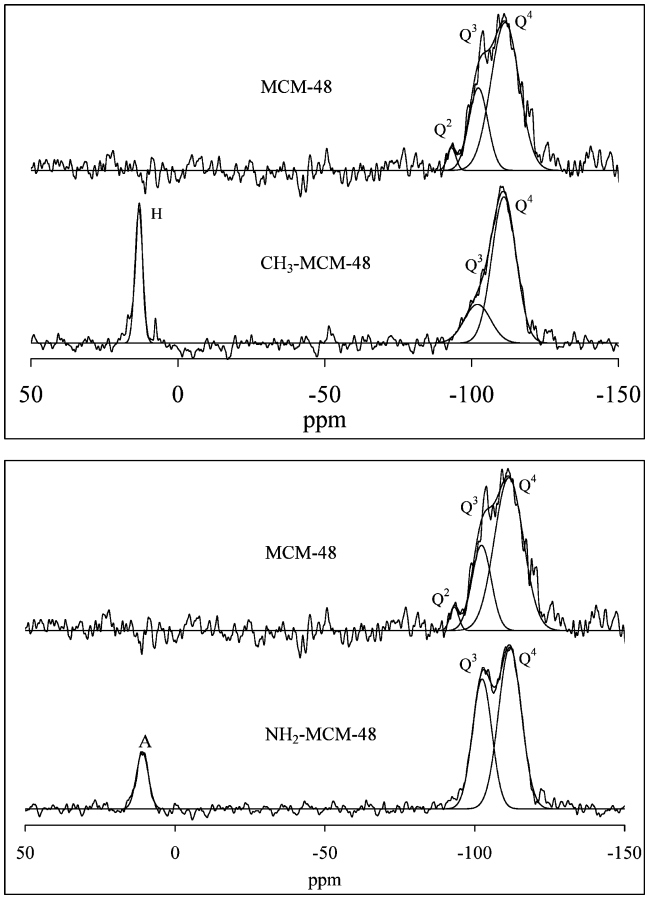

Figure 3. Solid state ^{29}Si MAS NMR spectra of MCM-48, CH_3-MCM-48, and NH_2-MCM-48.

extended length of the grafted species, that is, 0.74 nm in the case of trimethylsilane.[50] This, however, assumes close packing of the surface-grafted species. If close packing is not achieved, the grafted moieties are not sterically forced to fully extend normal to the surface. The moieties have bending degrees of freedom, resulting in a smaller total reduction in pore diameter, as observed in the present study and also by Zhao et al. For NH_2-MCM-48, the reduction in average pore diameter was ~0.2 nm, less than expected for attachment of fully extended 3-aminopropyldimethylsilane groups, which are larger than the trimethylsilane groups. The smaller than expected reduction in pore diameter can also be attributed to a low surface coverage for the aminopropylsilane groups.

The solid-state ^{29}Si NMR spectrum of MCM-48 (Figure 3) contains two distinct peaks, one at ~ -103 ppm and another at ~ -112 ppm. These are assigned as surface vicinal silanol groups (Q^3) and framework silica (Q^4), respectively. A further peak discernible at ~ -93 ppm is attributed to the surface geminal silanol groups (Q^2). These peak positions are consistent with those reported for the silica species in mesoporous molecular sieves.[5,46,51] The CH_3-MCM-48 spectrum (Figure 3) is significantly different from that for unmodified MCM-48. An additional peak at 13 ppm, not present in the MCM-48 spectrum, is attributed to the surface-grafted species. The position of this additional peak, labeled H, is consistent with the peak position reported for chemically grafted trimethylsilane moieties on other mesoporous materials.[47,50] The NH_2-MCM-48 spectrum (Figure 3) also contains an additional peak not present in the MCM-48 spectrum, which is at a chemical shift of ~11 ppm and is labeled A. This is attributed to the surface-

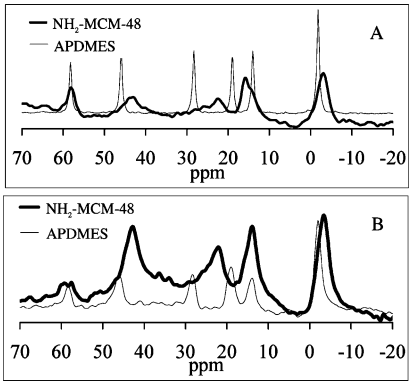

Figure 4. ^{13}C NMR spectra (A) SP and (B) CP of NH_2-MCM-48 (MAS) and APDMES (static).

grafted aminosilane groups. No peak was detected at −93 ppm, the position of the Q^2 signal in the MCM-48 spectrum.

Interestingly, surface functionalization with HMDS led to a significant decrease in the height of the Q^3 relative to the Q^4 peaks an effect previously reported to occur after the surface modification of other mesoporous materials.[47,50,52] Wouters et al. found that the decrease in the relative area under the Q^3 peak corresponds to the area under the new peak (H) because of the surface-grafted moieties and suggested that there is a one-to-one conversion of silanol groups (Q^3) to siloxane groups (Q^4).[52] This drop in the Q^3/Q^4 ratio, together with the position of the additional peak in the CH_3-MCM-48 spectrum, are strong evidence for the covalent attachment of trimethylsilane moieties after treatment with HMDS. However, functionalization with APDMES did not result in significant changes to the relative heights of the Q^3 and Q^4 peaks at about −103 and −112 ppm, respectively.

To gain further insight into the nature of the attachment and of the groups contributing to peak A in the NH_2-MCM-48 ^{29}Si solid-state MAS NMR spectrum (Figure 3), static ^{29}Si of liquid APDMES (not shown), solid-state ^{13}C MAS of NH_2-MCM-48, and static ^{13}C of APDMES liquid, both in SP mode and with CP (Figure 4), NMR spectra were also acquired. The ^{29}Si NMR spectrum of liquid APDMES showed a major peak with a chemical shift of ∼17 ppm due to the APDMES molecules, and a secondary smaller peak at ∼9 ppm believed to have resulted from reaction of APDMES molecules with the walls of the glass tube containing the sample for analysis or possibly deterioration byproducts due to contact with moist air. The ^{13}C NMR spectra, both in CP and SP mode, of liquid APDMES showed six peaks, which were assigned to the six different kinds of carbon present in APDMES (Figure 5). This was done by comparing the chemical shift to that reported for a similar molecule, 3-aminopropyltriethoxisilane (APTES).[53] The peak assignments for APTES and APDMES are listed in Table 2.

Following surface modification, carbon atoms with four different chemical environments should be present in the attached moiety resulting from reaction of APDMES (Figure 5). The resulting chemical shifts would be expected to be more shielded than those of the corresponding carbon atoms in APDMES because the ethoxy part of the molecule would be replaced by a siloxane bridge to the framework silica. However the ^{13}C spectra of NH_2-MCM-48 showed five separate peaks, including one peak at ∼15 ppm with a discernible shoulder indicating two overlapping signals. Comparison of the SP and CP signals revealed that the position of this peak shifted from 16 to 14 ppm, while all other peak positions remained constant, confirming that at ∼15 ppm two signals in close proximity were overlapping. The total number of different carbon signals was,

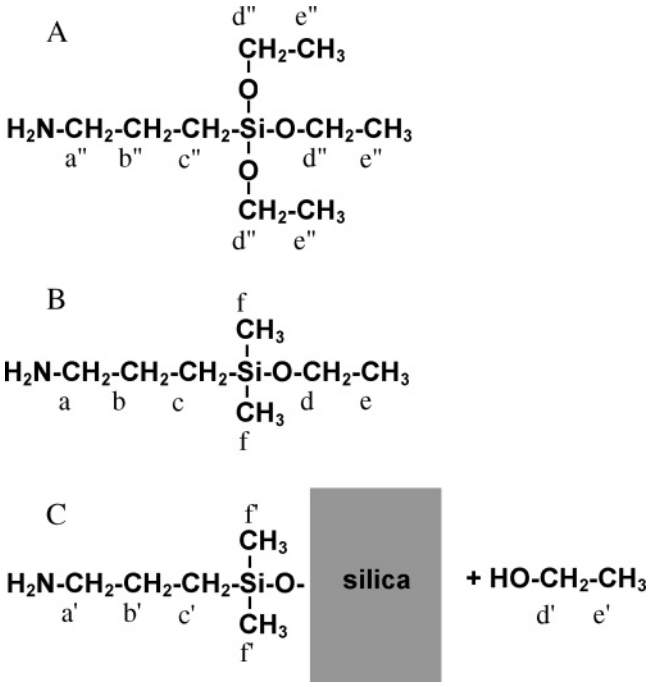

Figure 5. Chemical structure of (A) APTES, (B) APDMES, and (C) NH_2-MCM-48 with carbon molecules indexed for ^{13}C NMR assignments.

TABLE 2: ^{13}C Resonance Assignments (ppm) of APTES, APDMES, Ethanol, and NH_2-MCM-48[a]

	a, a′, a″	b, b′, b″	c, c′, c″	d, d′, d″	e, e′, e″	f, f ′, f ″
APTES	45	27	8	58	18	
APDMES	46	28	14	58	19	−2
ethanol				59	18	
NH_2-MCM-48	43	22	14	58	16	−3

[a] Labels taken from Figure 5.

therefore, six. Four of these signals were attributed to the carbon atoms in attached 3-aminopropyldimethylsilane groups by comparing their positions to the corresponding APDMES signals (Table 2). The remaining two peaks could be due to the presence of ethanol, a byproduct of the reaction. Although most of the ethanol would have been removed by the evacuation step following the surface modification reaction, a significant amount could have stayed physisorbed on the material. Ethanol in solvent ($CDCl_3$) has been reported to show ^{13}C resonances at ∼18 ppm for the CH_3 and ∼58 ppm for the $-CH_2OH$ group.[53] The carbons in this small molecule would be mobile and, therefore, would show a stronger signal in SP than in CP mode. This is consistent with the NMR results for NH_2-MCM-48: the signals at ∼58 and ∼16 ppm were more intense in the SP spectrum than in CP mode, whereas the other four peaks, attributed to attached APDMES groups, were more intense in the CP spectrum. The two peaks were, therefore, assigned to ethanol, and the difference in the position of the $-CH_3$ signal at ∼16 ppm compared to ∼18 ppm for ethanol in solution is possibly due to solvent effects and interaction of the ethanol with the surface.

All of the major signals in the NH_2-MCM-48 spectra, both in SP and CP mode, were assigned, although most of the peaks in the NH_2-MCM-48 spectra were fairly broad and may conceal any additional peaks arising from small amounts of APDMES deterioration products. Nevertheless, the ^{13}C NMR data from APDMES and NH_2-MCM-48 support a scheme for the reaction of APDMES with surface silanol groups to form covalently attached 3-aminopropyldimethylsilane moieties.

TABLE 3: Functional Group Concentrations and Densities for Unmodifed and Functionalized MCM-48[a]

	MCM-48	CH3-MCM-48	NH_2-MCM-48
[SiOH] (mmol/g)	6.9	3.5	6.3
$[Si(CH_3)_3]$ or [A] (mmol/g)		3.6	1.7
[SiOH] + ($[Si(CH_3)_3]$ or [A]) (mmol/g)	6.9	7.1	8.0
d_S (number/nm^2)	3.5	1.8	3.2
d_H or d_A (number/nm^2)		1.8	0.9
$d_S + (d_H$ or $d_A)$ (number/nm^2)	3.5	3.6	4.1

[a] [SiOH] = silanol group concentration, $[Si(CH_3)_3]$ = trimethylsilane group concentration, [A] = 3-aminopropyldimethylsilane group concentration, d_S = silanol group density, d_H = trimethylsilane group density, and d_A = 3-aminopropyldimethylsilane group density.

To obtain the concentrations of functional groups present in MCM-48, CH_3-MCM-48, and NH_2-MCM-48, we deconvoluted the ^{29}Si MAS NMR spectra with a least-squares fit using Gaussian normal distributions (3% standard error for CH_3-MCM-48 and NH_2-MCM-48 and 6% for MCM-48, Figure 3). The relative populations for the species were calculated from the areas under the fitted curves, and the functional group concentrations were determined from these results using a method reported by Wouters et al.[52] For example, in this method, the population of silanol groups per mol of MCM-48, is calculated from the relative population of silanol and geminal species, and divided by the weight per mol of MCM-48 (eq 1). The weight is derived from the relative populations and effective molecular weights (EMW) of the silanol, geminal, and siloxane species. The effective molecular weight of each species (EMW_{Q^i}) is defined as the sum of the molecular weight of the atoms contributing to each species, with the oxygen atoms in the siloxane bridges (Si−O−Si) that connect the species counted by half.

$$[\mathrm{SiOH}] = \frac{2 \times \%Q^2 + \%Q^3}{\sum (\%Q^i \times \mathrm{EMW}_{Q^i})} \quad (1)$$

where [SiOH] is the silanol group concentration in mol/g and % Q^i is the relative population of species Q^i (Q^2, Q^3, and Q^4). For CH_3-MCM-48 and NH_2-MCM-48, the trimethylsilane and 3-aminopropyldimethylsilane concentrations were determined in a similar manner. The functional group densities, shown in Table 3, were obtained by multiplying the concentrations by Avogadro's constant, to calculate the numbers of groups, and divided by the BET surface area, as done by Zhao et al.[50]

In the HMDS surface modification reaction, silanol groups react with HMDS in a 1:1 stoichiometric ratio. Therefore, after reaction, the sum of the trimethylsilane and unreacted silanol group concentrations is equal to the total silanol group concentration of the original material. The sum of the concentrations (7.1 mmol/g) was within 3% of the concentration on the original MCM-48 (6.9 mmol/g). The close agreement between these numbers is further evidence for the validity of the surface modification mechanism and for the covalent attachment of the trimethylsilane moieties.

A trimethylsilane group density, d_H, of 1.8 groups/nm^2 was determined for the CH_3-MCM-48. Zhao et al.[46] calculated the maximum theoretical density of trimethylsilane groups for MCM-41, based on each group taking up 0.43 nm^2, which corresponds to 2.33 groups/nm^2. Thus, the densities calculated here would correspond to a surface coverage of about 78%. However, this assumes a flat surface and does not take into account that groups attached around the narrow diameter of MCM-48 pores may have a lower maximum density because of steric hindrance. The highest surface coverages of trimethylsilane groups reported on MCM-41 from reactions in nonaqueous solvents are 1.9 and 1.79 groups/nm^2 using trimethylchlorosilane (TMCS)[50,54] and 1.51 groups/nm^2 with HMDS as a reagent.[36] Therefore, the group density achieved here was similar to the maximum densities reported previously.

The concentration of 3-aminopropyldimethylsilane groups, [A], (1.7 mmol/g) was more than 50% lower than the concentration calculated for trimethylsilane moieties (3.6 mmol/g). This is consistent with the reaction mechanism for APDMES proposed by White et al.,[31] wherein the conversion of surface silanol groups is limited by H bonding of the silanol groups with the amino end of attached 3-aminopropyldimethylsilane moieties. The sum of the concentrations, [A] and [SiOH], should still be equal to [SiOH] in the material prior to surface modification. However, the sum of the calculated concentrations was ~18% higher than the silanol group concentration on the original MCM-48. Amino groups have been reported to increase the likelihood of nucleophilic attack of the silica surface,[55] so the discrepancy may be due to additional silanol groups forming from hydrolysis of the material upon contact with moist air. Supporting evidence for hydrolysis was seen in the results of stability tests conducted on NH_2-MCM-48, which was found to be less hydrolytically stable that the original MCM-48 (see below).

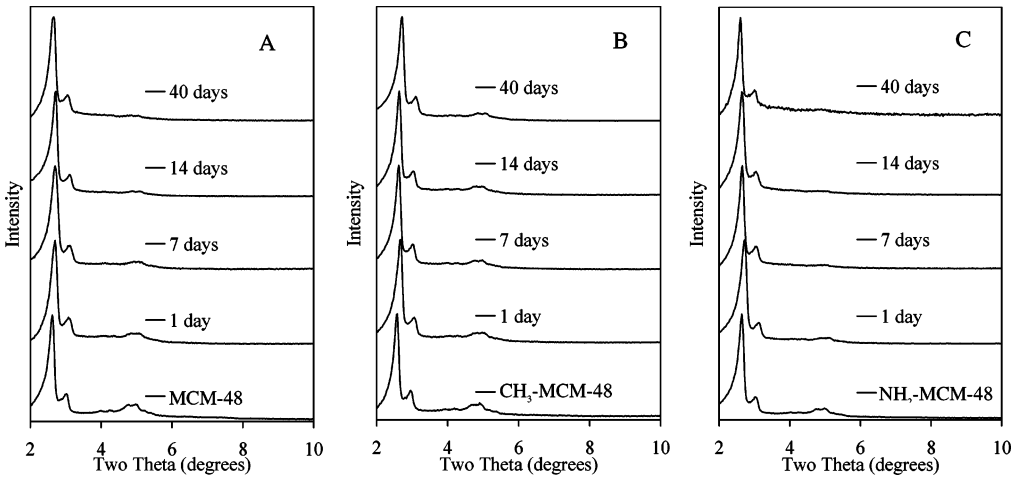

Figure 6. X-ray diffraction patterns for (A) MCM-48, (B) CH_3-MCM-48, and (C) NH_2-MCM-48 prior to and following 1−40 days in aqueous MES buffer at pH 6.

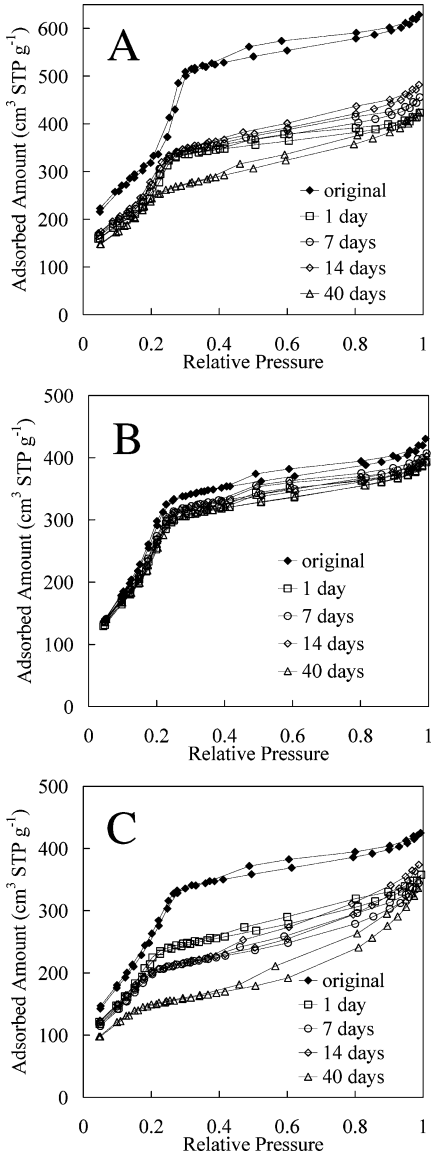

Figure 7. Nitrogen sorption isotherms for (A) MCM-48, (B) CH_3-MCM-48, and (C) NH_2-MCM-48 prior to and following 1−40 days in aqueous MES buffer at pH 6.

It has been shown recently that the use of an ethylenediamine (EDA) catalyst prior to APDMES addition resulted in the doubling of the concentration of the 3-aminopropyldimethylsilane groups attached to a nonporous silica powder and flat silica.[56] We have tested this method on samples of mesoporous and flat silica. For the flat silica, attachment of the APDMES was confirmed via atomic force microscopy; however, for the mesoporous silica, ^{13}C and ^{29}Si MAS NMR revealed only EDA present on the surfaces and no attachment of APDMES could be detected. The difference in performance of this reaction on mesoporous and flat silica may be due to insufficient removal of EDA from the mesopores because the vapor pressure would be significantly reduced in pores of this size (according to the Kelvin equation). Thus, a greater vacuum would be required to remove the EDA and ensure that only monolayer coverage remained within the pores.

The stability of MCM-48, CH_3-MCM-48, and NH_2-MCM-48 was tested by immersion in aqueous MES buffer at pH 6 for up to 40 days. For CH_3-MCM-48, the XRD patterns showed only slight changes from the original CH_3-MCM-48 after different periods in buffer (Figure 6). In addition to the two major peaks at low angles characteristic of MCM-48, all of the materials exhibited peaks at 3−5 degrees 2Θ, which have been associated with long-range order. A slight drop in the relative intensity of these long-range order peaks was detected once the material had been in contact with buffer. However, after 1 day in buffer the higher angle peak intensity showed little change, indicating that no further change in the material took place over the course of 40 days (Figure 6). This was in contrast to MCM-48 without surface modification, where immersion in buffer caused a marked decrease in higher angle peaks and, therefore, order of the structure. For NH_2-MCM-48, the XRD patterns also show that the two main peaks at low angles were retained for all of the samples, but the intensity of the higher angle peaks decreased with increasing immersion time (Figure 6). These peaks are associated with long-range order and, therefore, the changes indicate some loss of order in the materials due to immersion in buffer.

TABLE 4: Properties of MCM-48 Materials Determined by Nitrogen Sorption Prior to and Following 1−40 Days in Aqueous MES Buffer Solution at pH 6

time immersed in buffer solution (d)	single point pore volume at $p/p_0 \approx 0.99$ (cm^3/g)	BET surface area (m^2/g)
	MCM-48	
0	0.97	1181
1	0.65	901
7	0.70	960
14	0.75	1009
40	0.66	912
	CH_3-MCM-48	
0	0.67	1225
1	0.61	1016
7	0.63	1059
14	0.62	1058
40	0.61	1000
	NH_2-MCM-48	
0	0.66	1000
1	0.55	855
7	0.53	749
14	0.58	769
40	0.52	563

The loss of order detected in the XRD patterns was reflected in the nitrogen sorption isotherms for the NH_2-MCM-48 immersed in buffer (Figure 7), which were all shifted to significantly lower volumes of N_2 adsorbed in comparison with the original isotherm. In addition, the characteristic isotherm shape for MCM-48, with a step in the amount adsorbed between relative pressures of about 0.2−0.3, was almost completely lost for longer immersion times. The decrease in the specific amount of nitrogen adsorbed was reflected in the decreasing BET surface areas and pore volumes for NH_2-MCM-48 after immersion in buffer (Table 4). The maximum in the pore size distribution dropped significantly and shifted to smaller pore sizes, accompanied by a broadening of the peak (Figure 8). These results indicated that NH_2-MCM-48 was essentially not stable in pH 6 buffer under the conditions tested. The material showed significant changes in pore structure over the course of 40 days, while the regular structure of the underlying MCM-48 matrix was retained to some degree, but with some loss of long-range order. This effect may be due to the nature of the attached 3-aminopropyldimethylsilane moiety, where the conversion of surface silanol groups is limited by H bonding with the amino end, resulting in an increased likelihood of nucleophilic attack on the silica surface, enhancing the rate of hydrolysis.

The isotherms of the CH_3-MCM-48 stored in buffer were almost identical, independent of time, although all were slightly lower than those for the original CH_3-MCM-48 (Figure 7). This again is in marked contrast to MCM-48, where the amount of

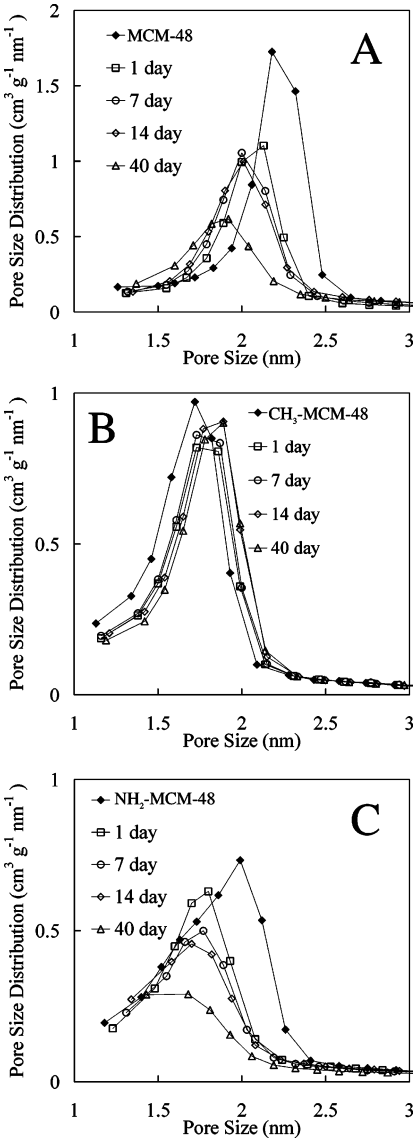

Figure 8. BJH pore size distributions for (A) MCM-48, (B) CH_3-MCM-48, and (C) NH_2-MCM-48 prior to and following 1−40 days in aqueous MES buffer at pH 6.

nitrogen adsorbed dropped significantly and the characteristic step in the isotherm became less pronounced after immersion in buffer. For CH_3-MCM-48, the maximum in the pore size distribution shifted to slightly larger values by about 0.1 nm upon contact with buffer, but showed little change with increasing time in buffer. The slight shift in pore diameter, and the slight decrease in adsorbed amounts visible in the isotherms, BET surface areas, and total pore volumes (Table 4), indicated initial changes in the material, such as a relaxation of the structure or structural rearrangement of the surface or possibly removal of deterioration product of nonreacted HMDS deposited in the pores during the surface modification reaction. Whatever the cause of these minor variations, because no further changes were seen, they did not appear to be related to instability of the material.

4. Conclusions

MCM-48 modified with hexamethyldisilazane (HMDS), CH_3-MCM-48, was found to retain the characteristic properties of the underlying silica material, contain ∼1.8 trimethylsilane groups per nm^2, and was essentially stable in pH 6 buffer solutions for 40 days, a major improvement in stability compared to unmodified MCM-48. The modified material shows promise for bioseparation applications, such as the separation of small biomolecules, peptides, and amino acids, where hydrophobic surfaces are important and the material is in contact with aqueous environments. NH_2-MCM-48, however, was found to contain ∼0.9 3-aminopropyldimethylsilane groups per nm^2 and, under the aqueous conditions tested, was seen to be less stable than the unmodified MCM-48. This effect may be due to the nature of the attached 3-aminopropyldimethylsilane moiety, where the conversion of surface silanol groups is limited by H bonding with the amino end, leading to a 50% lower functional group concentration and resulting in an increased likelihood of nucleophilic attack on the silica surface, enhancing the rate of hydrolysis. Therefore, HMDS is seen as a better functional species than APDMES for surface modification of MCM-48 for use in aqueous solutions.

Acknowledgment. S.B. would like to acknowledge the receipt of an Australian Postgraduate Award and CSIRO Postgraduate Scholarship. We all acknowledge access to infrastructure from the Particulate Fluids Processing Centre, a special research center of the Australian Research Council (ARC), and ARC Discovery Grant DP0451387.

References and Notes

(1) Broyer, M.; Valange, S.; Bellat, J. P.; Bertrand, O.; Weber, G.; Gabelica, Z. *Langmuir* **2002**, *18*, 5083.

(2) Beck, J. S.; Vartuli, J. C.; Roth, W. J.; Leonowicz, M. E.; Kresge, C. T.; Schmitt, K. D.; Chu, C. T.-W.; Olson, D. H.; Sheppard, E. W.; McCullen, S. B.; Higgins, J. B.; Schlenker, J. L. *J. Am. Chem. Soc.* **1992**, *114*, 10834.

(3) Kresge, C. T.; Leonowicz, M. E.; Roth, W. J.; Vartuli, J. C.; Beck, J. S. *Nature* **1992**, *359*, 710.

(4) Kim, J.; Kwak, J. H.; Jun, S.; Ryoo, R. *J. Phys. Chem.* **1995**, *99*, 16742.

(5) Xu, J.; Luan, Z. H.; He, H. Y.; Zhou, W. Z.; Kevan, L. *Chem. Mater.* **1998**, *10*, 3690.

(6) Oye, G.; Sjoblom, J.; Stocker, M. *Microporous Mesoporous Mater.* **1999**, *27*, 171.

(7) Schumacher, K.; Grun, M.; Unger, K. *Microporous Mesoporous Mater.* **1999**, *27*, 201.

(8) Gallis, K. W.; Eklund, A. G.; Jull, S. T.; Araujo, J. T.; Moore, J. G.; Landry, C. C. *Stud. Surf. Sci. Catal.* **2000**, *129*, 747.

(9) Morey, M. S.; Davidson, A.; Stucky, G. D. *J. Porous Mater.* **1998**, *5*, 195.

(10) Carrott, M. M. L. R.; Candeias, A. J. E.; Carrott, P. J. M.; Unger, K. K. *Langmuir* **1999**, *15*, 8895.

(11) Koyano, K. A.; Tatsumi, T.; Tanaka, Y.; Nakata, S. *J. Phys. Chem. B* **1997**, *101*, 9436.

(12) Zhao, X. S.; Lu, G. Q.; Hu, X. *Microporous Mesoporous Mater.* **2000**, *41*, 37.

(13) Edler, K. J.; White, J. W. *J. Mater. Chem.* **1999**, *9*, 2611.

(14) Igarashi, N.; Tanaka, Y.; Nakata, S.; Tatsumi, T. *Chem. Lett.* **1999**, *28*, 1.

(15) Kisler, J.; Stevens, G. W.; O'Connor, A. J. In *Proceedings of the 13th International Zeolite Conference: Zeolites and Mesoporous Materials at the Dawn of the 21st Century.* Montpellier, France, 2001; Galarneau, A., Di Renzo, F., Fajula, F., Vedrine, J., Eds.; Elsevier: Montpellier, France, 2001.

(16) Van der Voort, P.; Mathieu, M.; Vansant, E. F. In *Proceedings of the 13th International Zeolite Conference: Zeolites and Mesoporous Materials at the Dawn of the 21st Century*. Montpellier, France, 2001; Galarneau, A., Di Renzo, F., Fajula, F., Vedrine, J., Eds.; Elsevier: Montpellier, France, 2001.

(17) Yamamoto, K.; Tatsumi, T. *Microporous Mesoporous Mater.* **2001**, *44*, 459.

(18) Yang, J.; Daehler, A.; Stevens, G. W.; O'Connor, A. J. In *Nanoporous Materials III*, Canada, June 2002; Sayari, A., Jaroniec, M., Eds.; Elsevier: Canada, 2002.

(19) Zhao, X. S.; Audsley, F.; Lu, G. Q. *J. Phys. Chem. B.* **1998**, *102*, 4143.

(20) Landau, M. V.; Varkey, S. P.; Herskowitz, M.; Regev, O.; Pevzner, S.; Sen, T.; Luz, Z. *Microporous Mesoporous Mater.* **1999**, *33*, 149.

(21) Cassiers, K.; Linssen, T.; Mathieu, M.; Benjelloun, M.; Schrijnemakers, K.; Van Der Voort, P.; Cool, P.; Vansant, E. F. *Chem. Mater.* **2002**, *14*, 2317.
(22) Davidson, A. *Curr. Opin. Colloid Interface Sci.* **2002**, *7*, 92.
(23) Chen, L. Y.; Horiuchi, T.; Mori, T.; Maeda, K. *J. Phys. Chem. B* **1999**, *103*, 1216.
(24) Yu, J.; Shi, J. L.; Chen, H. R.; Yan, J. N.; Yan, D. S. *Microporous Mesoporous Mater.* **2001**, *46*, 153.
(25) Kim, J.; Jun, S.; Ryoo, R. *J. Phys. Chem. B* **1999**, *103*, 6200.
(26) Stein, A.; Melde, B. J.; Schroden, R. C. *Adv. Mater.* **2000**, *12*, 1403.
(27) Kisler, J.; Gee, M. L.; Stevens, G. W.; O'Connor, A. J. *Chem. Mater.* **2003**, *15*, 619.
(28) Lim, M. H.; Stein, A. *Chem. Mater.* **1999**, *11*, 3285.
(29) Kisler, J. M.; Stevens, G. W.; O'Connor, A. J. *Mater. Phys. Mech.* **2001**, *4*, 89.
(30) Tatsumi, T.; Koyano, K. A.; Tanaka, Y.; Nakata, S. *J. Porous Mater.* **1999**, *6*, 13.
(31) White, L. D.; Tripp, C. P. *J. Colloid Interface Sci.* **2000**, *232*, 400.
(32) Hair, M. L.; Tripp, C. P. *Colloids Surf., A* **1995**, *105*, 95.
(33) Tripp, C. P.; Hair, M. L. *Langmuir* **1992**, *8*, 1120.
(34) Tripp, C. P.; Hair, M. L. *Langmuir* **1995**, *11*, 149.
(35) Hertl, W.; Hair, M. L. *J. Phys. Chem.* **1971**, *75*, 2181.
(36) Anwander, R.; Nagl, I.; Widenmeyer, M.; Engelhardt, G.; Groeger, O.; Palm, C.; Roser, T. *J. Phys. Chem. B* **2000**, *104*, 3532.
(37) Yoshitake, H.; Yokoi, T.; Tatsumi, T. *Bull. Chem. Soc. Jpn.* **2003**, *76*, 847.
(38) Matsumoto, A.; Tsutsumi, K.; Schumacher, K.; Unger, K. K. *Langmuir* **2002**, *18*, 4014.
(39) Peng, Q.; Yang, Y.; Yuan, Y. *J. Mol. Catal. A: Chem.* **2004**, 219, 175.
(40) Schmidt, R.; Stocker, M.; Akporiaye, D.; Torstad, E. H.; Olsen, A. *Microporous Mater.* **1995**, *5*, 1.
(41) Brunauer, S.; Emmett, P. H.; Teller, E. *J. Am. Chem. Soc.* **1938**, *60*, 309.
(42) Kruk, M.; Jaroniec, M. *Chem. Mater.* **2000**, *12*, 222.
(43) Barrett, E. P.; Joyner, L. G.; Halenda, P. P. *J. Am. Chem. Soc.* **1951**, *73*, 373.
(44) Webb, P. A.; Orr, C. *Analytical Methods in Fine Particle Technology*; Micromertics Instrument Corporation: Norcross, 1997.
(45) Drechsler, A.; Separovic, F. *IUBMB Life* **2003**, *55*, 515.
(46) Zhao, X.; Lu, G. Q.; Whittaker, A. K.; Millar, G. J.; Zhu, H. Y. *J. Phys. Chem. B* **1997**, *101*, 6525.
(47) Sutra, P.; Fajula, F.; Brunel, D.; Lentz, P.; Daelen, G.; Nagy, J. B. *Colloids Surf., A* **1999**, *158*, 21.
(48) Kruk, M.; Jaroniec, M. *Chem. Mater.* **2001**, *13*, 3169.
(49) Kruk, M.; Jarioniec, M.; Sayari, A. *Langmuir* **1997**, *13*, 6267.
(50) Zhao, X. S.; Lu, G. Q. *J. Phys. Chem. B* **1998**, *102*, 1556.
(51) Gallis, K. W.; Landry, C. C. *Chem. Mater.* **1997**, *9*, 2035.
(52) Wouters, B. H.; Chen, T.; Dewilde, M.; Grobet, P. J. *Microporous Mesoporous Mater.* **2001**, *44*−*45*, 453.
(53) SDBSWeb, Integrated Spectral Data Base System for organic compounds, http://www/aist/go.jp/riodb/May2002. National Institute of Advanced Industrial Science and Technology.
(54) Jaroniec, C.; Kruk, M.; Jaroniec, M.; Sayari, A. *J. Phys. Chem. B* **1998**, *102*, 5503.
(55) Blitz, J. P.; Shreedhara Murthy, R. S.; Leyden, D. E. *J. Colloid Interface Sci.* **1998**, *126*, 387.
(56) Kanan, S. M.; Tze, W. T. Y.; Tripp, C. P. *Langmuir* **2002**, *18*, 6623.